MECSOL 2022 - Proceedings of the 8th International Symposium on Solid Mechanics
M.L. Bittencourt, J. Labaki, L.C.M. Vieira Jr. and E. Mesquita (Editors), Campinas SP, Brazil, October 17th to 19th, 2022

Effects of controlling stress field evolution in nonlinear poroelastic problems on the efficiency of iteratively-coupled algorithms

José Luís Medeiros Thiesen[1,3], Bruno Klahr [1], Otávio Teixeira Pinto[1], Thiago André Carniel[2], Eduardo Alberto Fancello[1,3]

[1] GRANTE - Department of Mechanical Engineering, Federal University of Santa Catarina, Florianópolis, Santa Catarina, Brazil
[2] LaTEM - Laboratory of Process and Technology in Materials, Polytechnic School, Community University of Chapecó Region, Chapecó, Santa Catarina, Brazil.
[3] LEBm - University Hospital, Federal University of Santa Catarina, Florianópolis, Santa Catarina, Brazil.

Coupled poroviscoelastic models, that are widely used to investigate biomechanics of hydrated soft biological tissues, may present distinct coupling strength arising from constitutive and geometrical parameters of each particular case. Regarding the coupled solution, the present study compares the effects on the computational performance of the monolithic and four iteratively-coupled solution schemes in the loading evolution controlling case within the context of soft biological tissues. To this end, a three-dimensional finite element model representing a force controlled confined compression was performed. The results highlight that the fixed-stress scheme and the monolithic one are well-suited methods for numerical experiments involving stress field control.

Keywords: Poroviscoelasticity, finite-strains, finite element method, monolithic, iteratively-coupled

INTRODUCTION

Poroelasticity theories have been widely used to model problems involving mechanics of porous media, such as those presented in biomechanics (Mow et.al., 1980; Ateshian and Weiss, 2010; Khayyeri et. al., 2015) and geomechanics (Biot, 1941, 1957; Kim et. al., 2011a). In the former case, the understanding of how the interactions of the interstitial fluid and its surrounding solid phase occur may bring essential information about the behaviour of hydrated soft biological tissues (Ehret et.al., 2017). In order to consider the large deformations and an additional dissipation intrinsic to the solid phase, finite-strain poroviscoelastic models (biphasic models) can be taken into consideration.

Considering biphasic models based on the Darcy's law to model the fluid flow in soft biological tissues, a wide range of permeability values can be found in literature. The choice of this parameter's value strongly affects the numerical coupling between the kinematics (displacement) and the fluid diffusion (pore pressure), raising concerns about the numerical performance of coupled solution schemes.

Considering finite-strain poroviscoelastic problems, the coupled solution is generally obtained by two well-known strategies: monolithic and iteratively-coupled (staggered-type) (Kim et. al., 2011a; Yi et.al. , 2017). While the monolithic scheme solves the coupled equations simultaneously at each time increment, the iteratively-coupled schemes split the biphasic problem into two subproblems: one related to the mechanical equilibrium and the other regarding the conservation of mass. At each time increment, the nonlinear subproblems are solved sequentially, until a certain convergence criterion is satisfied. Both strategies have their advantages and disadvantages. Although the monolithic approach is unconditionally stable and convergent, its resulting non symmetry makes it computationally costly and may require preconditioners and robust linear solvers (Hirabayashi and Iwamoto, 2018; Li and Wang, 2018). On the other hand, iteratively-coupled schemes result in two smaller symmetric system of equations, but may be limited due to the lack of stability and convergence issues (Kim et. al., 2011a; Kim et.al., 2011b,c).

In Klahr et. al. (2022), the authors compared the numerical performance of the monolithic approach with four types of iteratively-coupled schemes: *drained*, *undrained*, *fixed-strain* and *fixed-stress*. Although the monolithic seems to perform well for all displacement controlled compression cases studied, the authors concluded that there is no ideal scheme to solve such coupled problem, especially in the context of soft biological tissues, where the coupling strength of the model is far from self-evident.

Motivated by these aspects, the main goal of this paper is to complement the results found in Klahr et. al. (2022) by evaluating the computational performance of monolithic and iteratively coupled solution schemes in solving force-controlled confined compression problems (creep numerical experiments) in the context of soft biological tissues.

POROVISCOELASTICITY AT FINITE-STRAINS

Theoretical background

In poroviscoelastic models, the porous macroscopic level is considered to be in a homogenized condition, *i.e.*, the solid and fluid phases (at the microscale) are upscaled through volumetric fractions (porosity and solidity). In the case of soft biological tissues, the porous microstructure is modeled as a viscoelastic solid skeleton and a fluid flowing through the interconnected pores. In this class of models, there is no explicit separation of the solid and fluid media in the spatial configuration, with each point being treated as a solid-fluid mixture. The fundamental principles of the poroviscoelasticity theory presented henceforward are based on the classical references of Mow et.al. (1980), Dormieux et. al. (2006), Cheng (2016) and Serpieri and Travascio (2017).

Some important assumptions must be made in order to simplify the model and still adequately represent the soft biological tissues. The major hypotheses considered in this study are listed below:

1. The porous medium is saturated by the solid and fluid phases (biphasic model).
2. At the micro scale, both solid and fluid phases are incompressible. However, the overall porous medium is compressible, since there is fluid flow resulting from the deformation of the solid skeleton.
3. The total Cauchy stress tensor $\boldsymbol{\sigma}$ is defined by $\boldsymbol{\sigma} = \boldsymbol{\sigma}^{\mathrm{s}} + \boldsymbol{\sigma}^{\mathrm{f}}$, where $\boldsymbol{\sigma}^{\mathrm{s}}$ is the effective stress and $\boldsymbol{\sigma}^{\mathrm{f}} = -p\mathbf{I}$ is the hydrostatic stress resulting from the pore pressure p of the fluid phase. The effective stress $\boldsymbol{\sigma}^{\mathrm{s}}$ results from the well-known class of viscoelastic models, which will depend only on the deviatoric deformation history of the solid skeleton.

In the absence of inertial and body forces, the coupled problem in its strong form can be established:

$$\mathrm{div}_x\left(\boldsymbol{\sigma}^{\mathrm{s}} - p\mathbf{I}\right) = 0 \qquad \text{on } \Omega_x \tag{1a}$$

$$\mathrm{div}_x\left(\mathbf{v}^{\mathrm{s}} + \mathbf{w}\right) = 0 \qquad \text{on } \Omega_x \tag{1b}$$

$$\mathbf{u} = \bar{\mathbf{u}} \qquad \text{on } \partial\Omega_x|_{\mathrm{u}} \tag{1c}$$

$$\mathbf{t} = \bar{\mathbf{t}} \qquad \text{on } \partial\Omega_x|_{\mathrm{t}} \tag{1d}$$

$$p = \bar{p} \qquad \text{on } \partial\Omega_x|_{p} \tag{1e}$$

$$q^{\mathrm{f}} = \bar{q}^{\mathrm{f}} \qquad \text{on } \partial\Omega_x|_{q} \tag{1f}$$

where $\mathbf{w}$ is the relative fluid velocity, $\mathbf{v}^{\mathrm{s}}$ is the solid velocity and ν_x^{f} is the porosity of the medium. The relative fluid velocity is defined as

$$\mathbf{w} = \nu_x^{\mathrm{f}}\left(\mathbf{v}^{\mathrm{f}} - \mathbf{v}^{\mathrm{s}}\right), \tag{2}$$

where $\mathbf{v}^{\mathrm{f}}$ is the fluid velocity.

The equilibrium equations of the poroviscoelastic model are established by the conservation of linear and angular momentum, which in turn leads to Equation (1a) and to the symmetry of the total Cauchy stress tensor ($\boldsymbol{\sigma} = \boldsymbol{\sigma}^{\mathrm{T}}$), respectively. In addition, the conservation of mass for the biphasic domain results in Equation (1b). Finally, Equations (1c) to (1f) represent the Dirichlet and Neumann boundary conditions for both solid and fluid phases, where the vector $\bar{\mathbf{t}}$ is the external surface traction and the scalar $\bar{q}^{\mathrm{f}}$ is the external surface flux.

Constitutive modeling

In addition to the dissipation that arises from the fluid flow (represented by the classical Darcy's law), poroviscoelastic models exhibit a second dissipative response, arising from the intrinsic dissipation of the solid viscoelastic skeleton. In this work, the isotropic viscoelastic constitutive model of the solid skeleton was formulated within a consistent variational framework, which leads to a mathematically elegant and numerically robust tool to formulate constitutive updating for dissipative materials (Ortiz and Stainier, 1999; Fancello et.al., 2006; Carniel and Fancello, 2018). Given a time increment $\Delta t = t_{n+1} - t_n$, an incremental deformation gradient $\mathbf{F}_{n+1}$ and a set of incremental internal variables α_{n+1}, the main goal of the constitutive algorithm is to update the internal variables to their current state at t_{n+1} and evaluate the stress state by

$$\mathbf{P}^{\mathrm{s}}_{n+1} = \frac{\mathrm{d}\mathcal{P}_{\mathrm{red}}}{\mathrm{d}\mathbf{F}_{n+1}}, \quad \mathcal{P}_{\mathrm{red}}\left(\mathbf{F}_{n+1}\right) = \inf_{\alpha_{n+1}} \mathcal{P}_{\mathrm{inc}}\left(\mathbf{F}_{n+1}, \alpha_{n+1}\right), \tag{3}$$

where $\mathcal{P}_{\text{inc}}(\mathbf{F}_{n+1}, \alpha_{n+1}) = (\psi_{n+1} - \psi_n) + \Delta t\, \phi_{n+1}$ is an incremental potential defined as a function of the Helmholtz free energy $\psi(\mathbf{F}_{n+1}, \alpha_{n+1})$ and a dissipation potential $\phi(\mathbf{F}_{n+1}, \alpha_{n+1})$ that, in this case, takes the solid viscous dissipative behavior into account. The potential $\mathcal{P}_{\text{red}}$ is obtained by the minimization process of the incremental potential. The Helmholtz free energy potential ψ and the dissipation potential ϕ, alongside with the set of constitutive parameters used in the present study, are summarized in the numerical example section.

Regarding the fluid flow through the porous domain, the Darcy's law is used in this work. This law establishes a linear relation between the relative fluid velocity $\mathbf{w}$ and the spatial fluid pore pressure gradient $\text{grad}_x p$, given by

$$\mathbf{w} = -\mathbf{K}_x^{\text{f}} \,\text{grad}_x\, p, \tag{4}$$

where $\mathbf{K}_x^{\text{f}}$ is the spatial Darcy's permeability tensor. In this work, we considered an isotropic and constant permeability model, which can be defined in terms of the permeability constant κ,

$$\mathbf{K}_x^{\text{f}} = \kappa \mathbf{I}. \tag{5}$$

DISCRETIZATION AND SOLUTION

Incremental formulation

In the present investigation, a mixed finite element framework is employed to solve the poroviscoelastic equations. In this case, given a time step $\Delta t = t_{n+1} - t_n$, the semi-discrete variational form (weak form) of the coupled problem (1) can be set as

$$\delta W_{n+1}^{\text{s}} = \int_{\Omega_x} \boldsymbol{\sigma}_{n+1}^{\text{s}} : \delta\mathbf{e}_{n+1}\, \text{d}\Omega_x - \int_{\partial\Omega_{x|\text{t}}} \bar{\mathbf{t}}_{n+1} \cdot \delta\mathbf{u}_{n+1}\, \text{d}\partial\Omega_x \Big|_{\text{t}} - \int_{\Omega_x} p_{n+1} \text{tr}\,(\delta\mathbf{e}_{n+1})\, \text{d}\Omega_x = 0, \forall \delta\mathbf{u}_{n+1} \in \mathcal{V}_{\delta u}^{\text{s}}, \tag{6a}$$

$$\delta W_{n+1}^{\text{f}} = \int_{\Omega_x} \delta p_{n+1} \text{div}_x \mathbf{v}_{n+1}^{\text{s}}\, \text{d}\Omega_x - \int_{\Omega_x} \text{grad}_x \delta p_{n+1} \cdot \mathbf{w}_{n+1}\, \text{d}\Omega_x + \int_{\partial\Omega_{x|q}} \delta p_{n+1} \bar{q}_{n+1}^{\text{f}}\, \text{d}\partial\Omega_x \Big|_{q} = 0, \forall \delta p_{n+1} \in \mathcal{V}_{\delta p}^{\text{f}}. \tag{6b}$$

where the tensor $\delta\mathbf{e}_{n+1} = \text{sym}\,(\text{grad}_x \delta\mathbf{u}_{n+1})$ is the incremental version of the variation of the Euler-Almansi strain tensor, $\text{tr}\,(\cdot)$ is the trace operator, and $\text{div}_x(\cdot)$ and $\text{grad}_x(\cdot)$ are the spatial divergence and the spatial gradient operators, respectively. Moreover, $\mathcal{V}_{\delta u}^{\text{s}}$ and $\mathcal{V}_{\delta p}^{\text{f}}$ represent the admissible spaces for the variations $\delta\mathbf{u}$ and δp, respectively.

In accordance to what was proposed in Klahr et. al. (2022), a fully-implicit solution procedure via Newton-Raphson method was employed to solve the set of coupled nonlinear equations (6) monolithically. For this reason, the linearization of (6) is required. Assuming that the traction $\bar{\mathbf{t}}_{n+1}$ is not a function of $\mathbf{u}_{n+1}$, the directional derivative of $\delta W_{n+1}^{\text{s}}$ in the direction of the increment $\Delta\mathbf{u}_{n+1}$ results in

$$\begin{aligned} D\delta W_{n+1}^{\text{s}}[\Delta\mathbf{u}_{n+1}] = \frac{\partial \delta W_{n+1}^{\text{s}}}{\partial \mathbf{u}_{n+1}} \cdot \Delta\mathbf{u}_{n+1} &= \int_{\Omega_x} \delta\mathbf{e}_{n+1} : \mathbb{C}_{x_{n+1}}^{\text{s}} : \Delta\mathbf{e}_{n+1}\, \text{d}\Omega_x \\ &+ \int_{\Omega_x} \boldsymbol{\sigma}_{n+1}^{\text{s}} : \left[\text{grad}_x^{\text{T}} \Delta\mathbf{u}_{n+1}\, \text{grad}_x \delta\mathbf{u}_{n+1}\right] \text{d}\Omega_x \\ &- \int_{\Omega_x} p_{n+1} \mathbf{I} : \left[\text{grad}_x^{\text{T}} \Delta\mathbf{u}_{n+1}\, \text{grad}_x \delta\mathbf{u}_{n+1}\right] \text{d}\Omega_x \\ &- \int_{\Omega_x} p_{n+1} \text{div}_x \delta\mathbf{u}_{n+1}\, \text{div}_x \Delta\mathbf{u}_{n+1}\, \text{d}\Omega_x, \end{aligned} \tag{7}$$

where the fourth order tensor $\mathbb{C}_{x_{n+1}}^{\text{s}}$ is the spatial elasticity modulus of the solid skeleton (Bonet and Wood, 2008). Assuming that the solid contribution of the Cauchy stress tensor $\boldsymbol{\sigma}_{n+1}^{\text{s}}$ and the prescribed external surface traction $\bar{\mathbf{t}}_{n+1}$ are not functions of the pore pressure p_{n+1}, the directional derivative of $\delta W_{n+1}^{\text{s}}$ in the direction of the increment Δp_{n+1} results in

$$D\delta W_{n+1}^{\text{s}}[\Delta p_{n+1}] = \frac{\partial \delta W_{n+1}^{\text{s}}}{\partial p_{n+1}} \Delta p_{n+1} = -\int_{\Omega_x} \Delta p_{n+1} \text{tr}\,(\delta\mathbf{e}_{n+1})\, \text{d}\Omega_x. \tag{8}$$

Considering the backward Euler integration method, the incremental solid velocity field is approximated by

$$\mathbf{v}_{n+1}^{\text{s}} = (\mathbf{u}_{n+1} - \mathbf{u}_n)\Delta t^{-1}. \tag{9}$$

Therefore, the linearization of $\delta W^{\mathrm{f}}_{n+1}$ results in

$$\begin{aligned} D\delta W^{\mathrm{f}}_{n+1}[\Delta\mathbf{u}_{n+1}] = \frac{\partial \delta W^{\mathrm{f}}_{n+1}}{\partial \mathbf{u}_{n+1}} \cdot \Delta\mathbf{u}_{n+1} = &- \int_{\Omega_x} \delta p_{n+1} \mathrm{tr}\left(\mathrm{grad}_x \mathbf{v}^{\mathrm{s}}_{n+1} \mathrm{grad}_x \Delta\mathbf{u}_{n+1}\right) \mathrm{d}\Omega_x \\ &+ \int_{\Omega_x} \frac{1}{\Delta t} \delta p_{n+1} \mathrm{div}_x \Delta\mathbf{u}_{n+1} \, \mathrm{d}\Omega_x \\ &+ \int_{\Omega_x} \delta p_{n+1} \mathrm{div}_x \mathbf{v}^{\mathrm{s}}_{n+1} \mathrm{div}_x \Delta\mathbf{u}_{n+1} \, \mathrm{d}\Omega_x \\ &+ \int_{\Omega_x} \mathrm{grad}_x \delta p_{n+1} \cdot \left(\mathbb{K}^{\mathrm{f}}_{x_{n+1}} : \Delta\mathbf{e}_{n+1}\right) \mathrm{grad}_x p_{n+1} \, \mathrm{d}\Omega_x, \end{aligned} \tag{10}$$

$$D\delta W^{\mathrm{f}}_{n+1}[\Delta p_{n+1}] = \frac{\partial \delta W^{\mathrm{f}}_{n+1}}{\partial p_{n+1}} \Delta p_{n+1} = \int_{\Omega_x} \mathrm{grad}_x \delta p_{n+1} \cdot \left(\mathbf{K}^{\mathrm{f}}_{x_{n+1}} \mathrm{grad}_x \Delta p_{n+1}\right) \mathrm{d}\Omega_x, \tag{11}$$

where the fourth-order tensor $\mathbb{K}^{\mathrm{f}}_{x_{n+1}}$ is the spatial tangent permeability modulus (Ateshian and Weiss, 2010; Klahr et. al., 2022). Note that, in this linearization, the Darcy's law was considered to compute the relation between the relative velocity $\mathbf{w}$ and the pore pressure.

Numerical solution strategies

Considering the finite element method and the Newton-Raphson procedure to solve the system of nonlinear equations (6), the global system of equations can be stated as,

$$\begin{cases} \mathbf{K}^{\mathrm{uu}}_{n+1} \Delta\mathbf{q}_{n+1} + \mathbf{K}^{\mathrm{u}p}_{n+1} \Delta\mathbf{p}_{n+1} &= -\mathbf{r}^{\mathrm{u}}_{n+1} \\ \mathbf{K}^{p\mathrm{u}}_{n+1} \Delta\mathbf{q}_{n+1} + \mathbf{K}^{pp}_{n+1} \Delta\mathbf{p}_{n+1} &= -\mathbf{r}^{p}_{n+1} \end{cases}, \tag{12}$$

where the vectors $\mathbf{r}^{\mathrm{u}}_{n+1}$ and $\mathbf{r}^{p}_{n+1}$ represent the residual vectors defined by the discretization of equations (6a) and (6b), respectively. The matrices $\mathbf{K}^{\mathrm{uu}}_{n+1}$, $\mathbf{K}^{\mathrm{u}p}_{n+1}$, $\mathbf{K}^{p\mathrm{u}}_{n+1}$ and $\mathbf{K}^{pp}_{n+1}$ represent the tangent matrices of the Newton-Raphson method, obtained by the discretization of the equations (7), (8), (10) and (11), respectively. Finally, the vectors $\Delta\mathbf{q}_{n+1}$ and $\Delta\mathbf{p}_{n+1}$ represent the incremental nodal displacement and pore pressure, which are updated as

$$\mathbf{q}^{i+1}_{n+1} = \mathbf{q}^{i}_{n+1} + \Delta\mathbf{q}_{n+1} \qquad \text{and} \quad \mathbf{p}^{i+1}_{n+1} = \mathbf{p}^{i}_{n+1} + \Delta\mathbf{p}_{n+1}, \tag{13}$$

where the subscript i indicates the i-th iteration of the Newton-Raphson procedure (see more details in (Klahr et. al., 2022)).

Similar to other coupled multiphysics problems, the solution of such equations requires the application of consistent methods. Considering a fully-coupled solution, there are two main groups of methods commonly used to solve coupled equations of multiphysics problems. Firstly, the *monolithic* method consists in solving all the equations simultaneously within a single system of nonlinear equations, requiring the computation of all crossed-field linearizations. The consideration of the derivatives of the cross-fields significantly increases the size of the system of equations, and also results in ill-conditioning problems. Thus, this strategy requires robust methods for solving the linear system and efficient preconditioners. Secondly, there are *iteratively-coupled* schemes, which solve the system of nonlinear equations sequentially. The main goal of these iterative methods is to segregate the global problem into subproblems. Therefore, each sub-problem refers to a governing equation of the poroviscoelastics problem that is solved individually. In order to recover the fully-coupled solution, these methods introduce an additional staggered iteration loop inside each time step, and this procedure is maintained until a relative convergence criterion is fulfilled.

For the biphasic model, the subproblems are defined by the conservation of the linear momentum (6a) and by the conservation of mass (6b). In this context, four iteratively-coupled schemes are commonly considered: *drained*, *undrained*, *fixed-strain* e *fixed-stress*. These four iteratively-coupled methods used herein are extensively discussed in Klahr et. al. (2022).

NUMERICAL EXAMPLE

In order to compare the performance of different solution schemes in a stress-controlled case, a study with a three-dimensional numerical specimen was performed. Considering a soft biological tissues context, the geometrical and constitutive parameters were chosen according to the propositions presented in Klahr et. al. (2022). For all simulations, the

specimen height and cross section diameter were $h = 2$ mm and $d = 4$ mm, respectively. The mechanical behavior of the solid skeleton was assumed homogeneous and isotropic. In order to represent this behavior, a variational viscoelastic model was used. The specific potentials and constitutive parameters were chosen within the context of tendons' mechanics (Klahr et. al., 2022). Regarding the fluid flow, the Darcy's law was employed with an isotropic and constant permeability model. In this case, the permeability tensor depends on a single parameter κ. While for all simulations the mechanical response of solid skeleton was kept fixed, the parameter κ varied within the range of $1 \cdot 10^{-5}$ and $5 \cdot 10^{-3}$ mm^4/Ns. It is important to emphasize that the units of all constitutive parameters used in the numerical simulations was chosen in order to reduce the differences among order of magnitudes between the multiphysics problems, mitigating ill-conditioning problems within the linear system.

In order to consider the symmetry of the problem, only one quarter of the specimen was simulated. For the purpose of a creep numerical experiment, a controlled compressive force was applied at 0.6 N/s until 60 N, and kept fixed for $t = 100$ seconds. In the case of confined compression with the force being applied through a rigid permeable plate, fluid flow is allowed only at the top surface. This condition was considered by applying a zero pore pressure boundary condition at the top boundaries of the specimen. Figure 1 shows a schematic representation of the problem. This is a benchmark case in the literature of soft biological tissues and despite being simple it encompasses several numerical difficulties due to the low permeability of such tissues and the large deformations to which they are subjected.

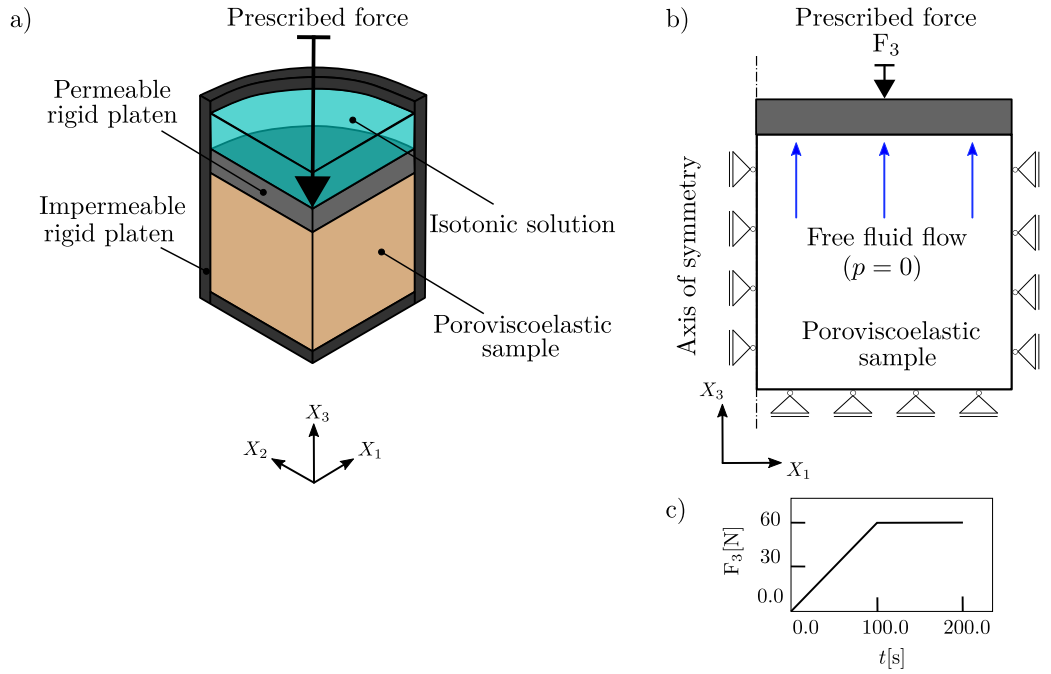

Figure 1 – Schematic representation of the numerical example. (a) Confined compression with a prescribed force. The sample was confined on a impermeable rigid chamber, thus, the fluid was allowed to flow only through the top surface (the force was prescribed through a permeable platen). (b) Two-dimensional scheme of the applied boundary conditions. (c) Load-control curve.

RESULTS AND DISCUSSIONS

This section aims to investigate the numerical results in the case of stress-control for the different solution methods developed in Klahr et. al. (2022). To this purpose, following the choices made in Klahr et. al. (2022), a confined compression model composed by 2400 mixed isoparametric hexaedral finite elements and a time increment of $\Delta t = 5$ s were considered in all analyses.

To solve the linear systems associated with the full Newton–Raphson algorithm, the sparse direct solver Pardiso was used (Bollhofer et. al., 2020). This is a robust library that handles with both symmetric and non-symmetric types of systems of linear equations. Concerning the convergence criterion used in the Newton-Raphson algorithm and the iteratively-coupled scheme, tolerance parameters on the order of 10^{-5} and 10^{-3} were adopted, respectively.

Although it is not explicitly presented, all the iteratively-coupled schemes considered in this work converged to the

monolithic results (Klahr et. al., 2022). Figure 2 presents the pore pressure and von Mises measure of total Cauchy stress fields at the instant of maximum applied force (time $t = 100$ s). These field plots refer to the solutions obtained for the permeability parameter $\kappa = 10^{-5}\text{mm}^4/\text{Ns}$. Note that, from this point on ($t > 100$ s), although the applied force remains constant, the axial displacement continues to evolve due to the creep phenomenon.

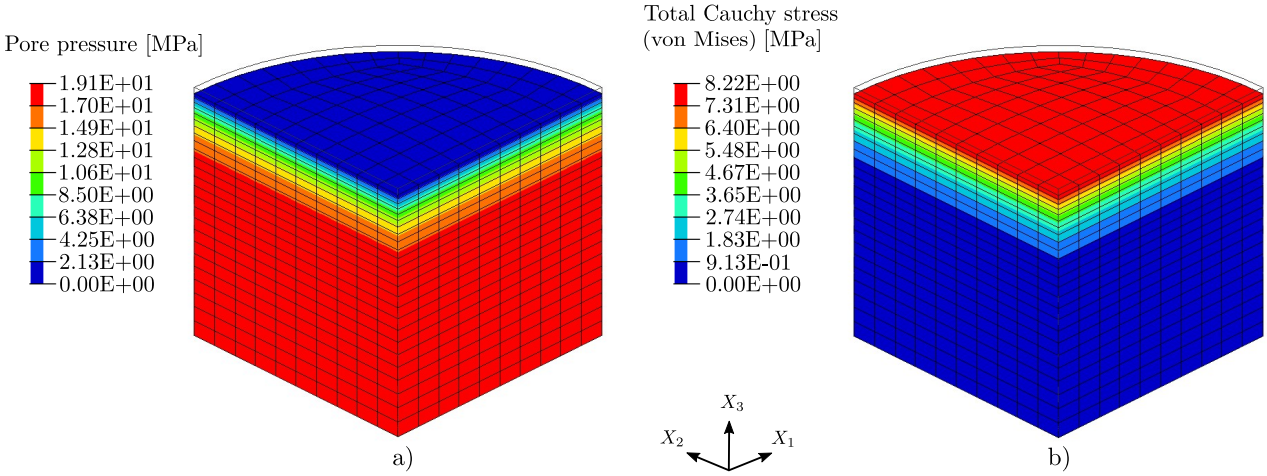

Figure 2 – Three-dimensional field results of the confined compression model. (a) Pore pressure field. (b) The von Mises measure of the total Cauchy stress. Results were obtained considering $\kappa = 10^{-5}\text{mm}^4/\text{Ns}$ at time $t = 100$ s.

In order to investigate the correlation between the poroviscoelastic response with the permeability parameter, Fig. 3 shows the axial displacement and pore pressure curves obtained in specific points and plotted over time. One can see that low permeability values imply a higher resistance of the fluid to flow, increasing the pore pressure and, consequently, its contribution to support the total applied force. Therefore, the permeability value is strongly correlated with the coupling between the mechanical balance and the mass conservation problem. In the case of controlling the force applied, we can note that low permeability values leads to a slow evolution of the axial displacement, delaying the creep phenomenon.

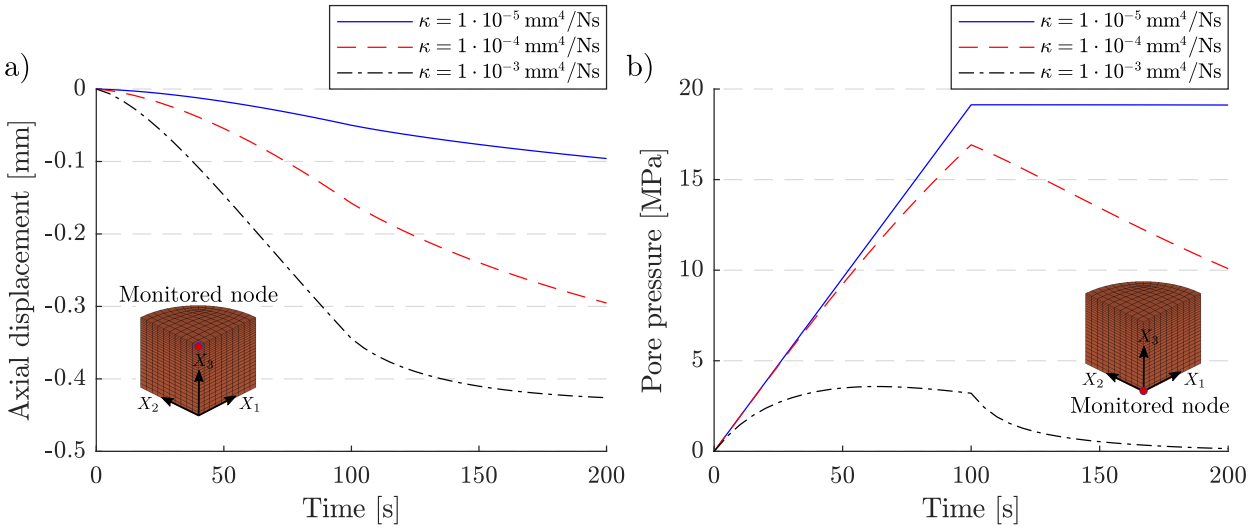

Figure 3 – Solution comparison of the confined compression for three different permeabilities κ (a) Reaction force on monitored area. (b) Pore pressure on the monitored point.

In line with the main goal of this paper, Fig. 4 shows a normalized processing time in order to compare the solutions among coupled schemes. This normalized processing time was calculated as the ratio between each processing time and the maximum processing time. In addition, for the iteratively-coupled schemes, we included the total number of sequential iterations between the subproblems to reach convergence.

We can verify that only the monolithic and the fixed-stress schemes achieved convergence for all permeabilities studied. Regarding the normalized processing time, the simulations show that while for low permeability values the monolithic performs better than the others, with the increase of permeability, the fixed-stress becomes the best one. Similar to observed by Klahr et. al. (2022), the fixed-strain and drained splits have shown lack of convergence on numerical simulations with low permeabilities. In this case, the undrained scheme has also revealed to be unstable for low permeabilities. For those cases, the stability is related to the choice of time integration method and the poroviscoelastic parameters, which could influence in the coupling strength of the problem (Kim et. al., 2011a; Kim et.al., 2011b,c). We note that all the solution schemes present a decrease in the processing time as the permeability value is increased (lower *coupling strength*).

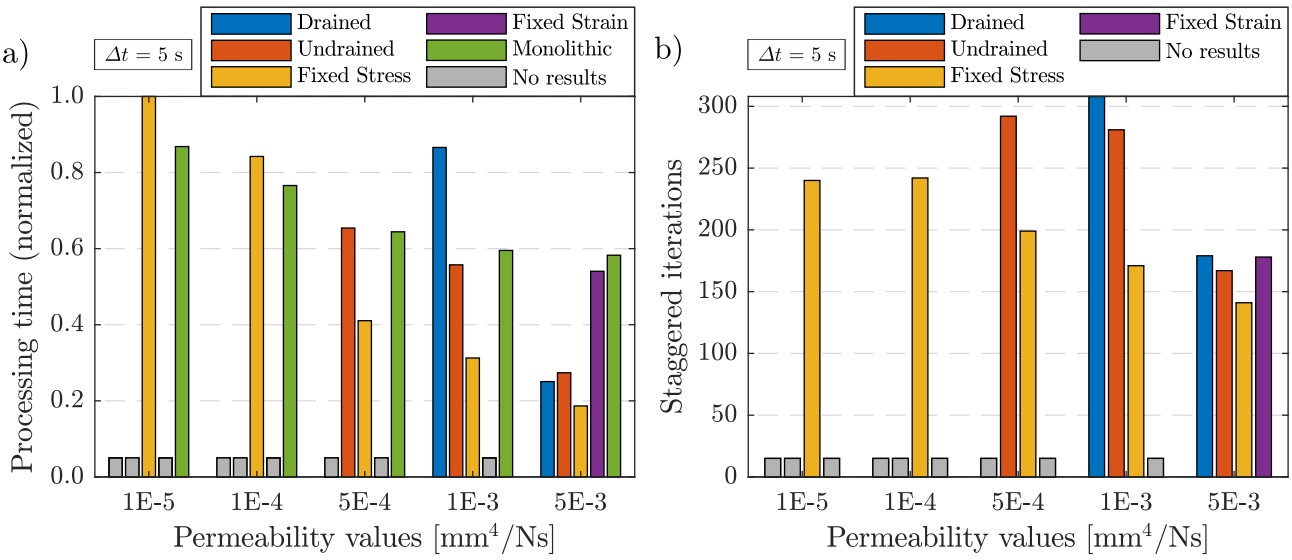

Figure 4 – Algorithmic results for the confined compression considering $\Delta t = 5$ s. (a) Normalized processing time. (b) Number of staggered iterations.

In addition to the normalized processing time, it becomes interesting to assess the number of iterations of the full Newton-Raphson algorithm. The monolithic scheme takes on average 3 iterations to achieve convergence in each time step. It is important to mention, however, that the loading step ($0 < t < 100$ s) represents the majority of these iterations. We can note that when the permeability decreases, the number of nonlinear iterations tends to increase, information that corroborates with the processing time of Fig. 4.

Regarding the iteratively-coupled schemes, Tab. 1 presents the number of Newton-Raphson iterations of each sub-problem. We can verify that when the value of the permeability constant increases, the total number of nonlinear iterations decreases, which is in agreement with the number of staggered iterations. In addition, it can be verified that the mechanical problem $\mathcal{M}$ requires a larger number of nonlinear iterations than fluid flow problem $\mathcal{F}$, a characteristic observed in all cases. However, it is important to emphasize that the number of iterations of each sub-problem is not directly proportional to the total processing time, since the mechanical problem is more computationally expensive due to the larger number of degrees of freedom.

FINAL REMARKS

The performance and suitability of a monolithic and four iteratively-coupled numerical schemes (drained, undrained, fixed-strain, and fixed-stress splits) to solve biphasic problems within the context of soft tissues biomechanics was studied in this article. This work complements the investigations pointed out by Klahr et. al. (2022), where the authors performed displacement-controlled analysis. For this purpose, a numerical confined compression case with controlling of the loading evolution was performed. Aiming to evaluate the ability of each solution method to solve the coupled poroviscoelastic problem, the normalized processing time and the number of staggered iterations of each iteratively-coupled schemes were compared, considering that all procedures should achieve the same final solution.

We can verify that the monolithic scheme and the fixed-stress split showed to be the most reliable, in the sense of capability of achieving convergence. With respect to processing time, while the monolithic is the fastest for low permeabilities, the fixed-stress algorithm is the most suitable for high permeabilities.

Table 1 – Total number of Newton-Raphson iterations for each iteratively-coupled method for each sub-problem in the confined compression case. Results for the time increment $\Delta t = 5$ s and for five permeabilities ($\kappa_1 = 1 \cdot 10^{-5}\,\mathrm{mm^4/Ns}$, $\kappa_2 = 1 \cdot 10^{-4}\,\mathrm{mm^4/Ns}$, $\kappa_3 = 5 \cdot 10^{-4}\,\mathrm{mm^4/Ns}$, $\kappa_4 = 1 \cdot 10^{-3}\,\mathrm{mm^4/Ns}$ and $\kappa_5 = 5 \cdot 10^{-3}\,\mathrm{mm^4/Ns}$) .

		κ_1	κ_2	κ_3	κ_4	κ_5
Drained	$\mathcal{M}$	–	–	–	796	220
	$\mathcal{F}$	–	–	–	465	179
Undrained	$\mathcal{M}$	–	–	590	490	234
	$\mathcal{F}$	–	–	294	281	167
Fixed-strain	$\mathcal{M}$	–	–	–	–	477
	$\mathcal{F}$	–	–	–	–	347
Fixed-stress	$\mathcal{M}$	1181	940	441	328	197
	$\mathcal{F}$	319	285	205	183	140

As addressed in Klahr et. al. (2022), iteratively-coupled schemes seem to perform well over the monolithic one for weak coupling cases (high permeability in this case). In addition, the iterative schemes may suffer from lack of convergence when the coupling strength increases. However, for the case of controlling the loading evolution, the fixed-stress split proved to be stable in all cases, while also obtaining good performance results.

Based on the numerical results presented in this paper, we conclude that in spite of the monolithic scheme remaining a viable choice for solving biphasic problems in a biomechanical context with high coupling strength, the fixed-stress scheme emerges as an excellent alternative in the case of controlling loading. Therefore, this study supports the conclusions of Klahr et. al. (2022), pointing out that there is no optimal scheme to solve poroviscoelastic problems and that the solution method must be chosen according to the case (boundary conditions, load profiles, constitutive and geometric parameters, and others).

ACKNOWLEDGMENTS

The authors would like to thank the following funding agencies: CAPES (Coordination for the Improvement of Higher Education Personnel), CNPq National Council for Scientific and Technological Development) and FAPESC (Foundation for Research and Innovation of the State of Santa Catarina, Grant No.: 2021TR000634).

REFERENCES

Biot, M.A., Willis, D.G., 1957, "The elastic coefficients of the theory of consolidation".

Biot, M.A., 1941, "General theory of three-dimensional consolidation", Journal of applied physics, 12 (2).

Ateshian, G.A., Weiss, J.A., 2010, "Anisotropic hydraulic permeability under finite deformation", Journal of biomechanical engineering, 132 (11), doi: 10.1115/1.4002588.

Bollhofer, M., Schenk, O., Janalik, R., Hamm, S., Gullapalli, K., 2020, "State-of-the-Art Sparse Direct Solvers." In: Grama, A., Sameh, A. (eds) Parallel Algorithms in Computational Science and Engineering. Modeling and Simulation in Science, Engineering and Technology, Birkhauser, Cham, doi: 10.1007/978-3-030-43736-7-1.

Bonet, J., Wood, R.D., 2008, "Nonlinear continuum mechanics for finite element analysis", Cambridge University Press, 2nd edition.

Carniel, T.A., Fancello, E.A., 2018, "A variational homogenization approach applied to the multiscale analysis of the viscoelastic behavior of tendon fascicles", Continuum Mechanics and Thermodynamics, 31(3):607-626,doi:10.1007/s00161-018-0714-y.

Cheng, A.H.D., 2016, "Theory and Applications of Transport in Porous Media", Springer International Publishing, Cham, ISBN 978-3-319-25200-1, doi: 10.1007/978-3-319-25202-5.

Dormieux, L., Kondo, D., Ulm, F.J., 2006, "Microporomechanics", John Wiley & Sons, Ltd, Chichester, UK, ISBN 9780470032008, doi:10.1002/0470032006.

Ehret, A.E., Bircher, K., Stracuzzi, A., Marina, V., Zündel, M., Mazza, E., 2017, "Inverse poroelasticity as a fundamental mechanism in biomechanics and mechanobiology", Nature Commun., 8(1):1-10. doi:10.1038/s41467-017-00801-3.

Fancello, E.A., Ponthot, J.P., Stainier, L., 2006,"A variational formulation of constitutive models and updates in non-linear finite viscoelasticity", International Journal for Numerical Methods in Engineering, 65(11):1831–1864,doi: 10.1002 /nme.1525.

Hirabayashi, S., Iwamoto, M., 2018, "Finite element analysis of biological soft tissue surrounded by a deformable membrane that controls transmembrane flow", Theor Biol Med Model., 15(1):21. doi:10.1186/s12976-018-0094-9

Khayyeri, H., Gustafsson, A., Heuijerjans, A., et al., 2015, "A fibre-reinforced poroviscoelastic model accurately describes the biomechanical behaviour of the rat achilles tendon", PLoS One, 10(6):1-18. doi:10.1371/journal.pone.0126869

Kim, J., Tchelepi, H.A., Juanes, R., 2011, "Stability, accuracy, and efficiency of sequential methods for coupled flow and geomechanics", SPE J., 16(02):249-262, doi:10.2118/119084-PA.

Kim, J., Tchelepi, H.A., Juanes, R., 2011, "Stability and convergence of sequential methods for coupled flow and geomechanics: drained and undrained splits", Comput Methods Appl Mech Eng., 200(23-24):2094-2116, doi:10.1016/j.cma.2011.02.011.

Kim, J., Tchelepi, H.A., Juanes, R., 2011, "Stability and convergence of sequential methods for coupled flow and geomechanics: fixed-stress and fixed-strain splits", Comput Methods Appl Mech Eng., 200(13-16):1591-1606, doi:10.1016/j.cma.2010.12.022.

Klahr, B., Medeiros Thiesen, J.L., Teixeira Pinto, O., Carniel, T.A., Fancello, E.A., 2022, "An investigation of coupled solution algorithms for finite-strain poroviscoelasticity applied to soft biological tissues", Int. J. Numerical Methods Eng., 123(9): 2112– 2141, doi:10.1002/nme.6928.

Li, G.,Wang, K., 2018, "Stabilized low-order explicit finite element formulations for the coupled hydro-mechanical analysis of saturated poroelastic media", Transp Porous Media., 124(3):1035-1059. doi:10.1007/s11242-018-1109-z

Mow, V.C., Kuei, S.C., Lai, W.M., Armstrong, C.G., 1980, "Biphasic creep and stress relaxation of articular cartilage in compression: theory and experiments", Journal of biomechanical engineering, 102(1), 73:84, doi:10.1115/1.3138202.

Ortiz, M., Stainier, L., 1999, "The variational formulation of viscoplastic constitutive updates", Computer Methods in Applied Mechanics and Engineering, 7825(98):419-444, doi:10.1016/S0045-7825(98)00219-9.

Serpieri, R., Travascio, F., 2017, "Variational Continuum Multiphase Poroelasticity", Advanced Structured Materials, Springer Singapore, Singapore, vol. 67, ISBN 978-981-10-3451-0, doi: 10.1007/978-981-10-3452-7.

Yi, S-Y., Bean, M.L., 2017, "Iteratively coupled solution strategies for a four-field mixed finite element method for poroelasticity", Int J Numer Anal Methods Geomech., 41(2):159-179, doi:10.1002/nag.2538.

RESPONSIBILITY NOTICE

The authors are the only parties responsible for the printed material included in this paper.